13th Scientific/Research Symposium with International Participation
„METALLIC AND NONMETALLIC MATERIALS“, B&H, 27th May 2021

STUDY OF THERMAL PROPERTIES AND MICROSTRUCTURE OF THE Sn-Ag ALLOYS

Dragan Manasijević, Ljubiša Balanović, Ivana Marković,
Milan Gorgievski, Uroš Stamenković
University of Belgrade, Technical Faculty in Bor
Bor
Serbia

Duško Minić, Aleksandar Đorđević
University of Priština, Faculty of Technical Science
Kosovska Mitrovica
Serbia

Keywords: Sn-Ag system, microstructure, thermal conductivity

ABSTRACT
Thermal properties and microstructure of the Sn-10% Ag and Sn-20% Ag alloys were experimentally investigated in this study. Melting behavior of the alloys were studied using differential scanning calorimetry (DSC). Microstructure of the alloys was analyzed by optical microscopy. The xenon-flash method was used for the measurements of thermal diffusivity, specific heat capacity and thermal conductivity in the temperature range from 25 to 150 °C. The obtained results were compared with the results of thermodynamic calculation and literature data and relatively good agreement is observed.

1. INTRODUCTION
The multicomponent alloys based on Sn and Ag represent basis for development of Pb- free solders [1].
It is known that the Sn-Ag alloys have superior mechanical properties such as high strength and creep resistance [2]. Regarding the investigations of thermophysical properties, Fima [3] studied density and surface tension of liquid Sn-Ag alloys. Thermal, electrical, microstructure properties and microhardness of the eutectic Sn-3.5wt.%Ag alloy were investigated by Meydaneri et al. [4]. Çadırlı et al. [5] investigated dependence of electrical and thermal conductivity on temperature in directionally solidified Sn–3.5 wt% Ag eutectic alloy.
The calculated phase diagram of the Ag-Sn system [6] is given in Fig. 1. Beside liquid, (Ag) and (Sn) solid solution phases it includes ζ and Ag_3Sn intermediate phases. Three invariant reactions occur in this system. Two of them, appearing at high temperatures, are (Ag)+liquid→ ζ and ζ +liquid→ Ag_3Sn peritectic reactions. The Sn-rich alloys encounter the liquid→(Sn)+ Ag_3Sn eutectic reaction, which appears at 221.7 °C. Eutectic alloy has 3.5 wt.% of Ag.

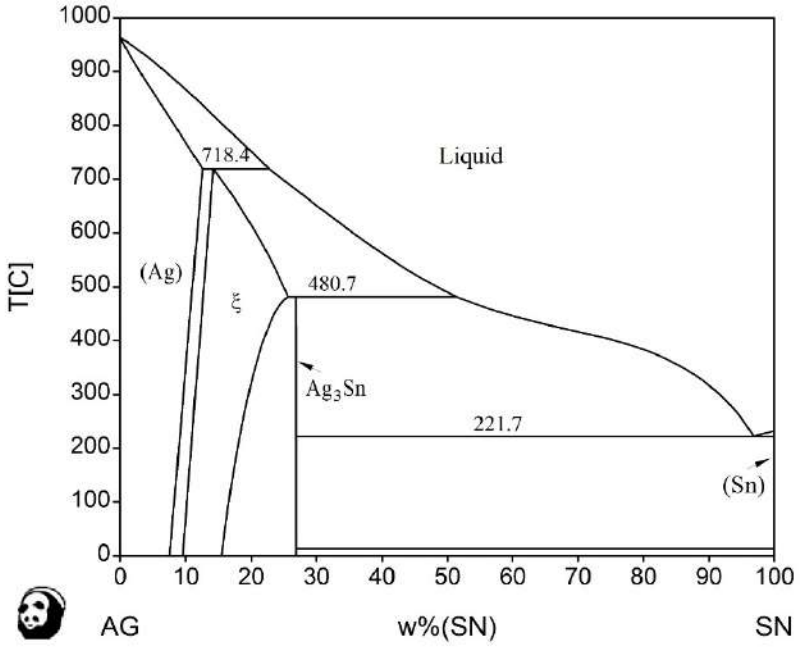

Figure 1. Calculated phase diagram of the Ag-Sn system using optimized thermodynamic data from [6]

The previous studies of mechanical and thermal properties were mainly focused on the Sn–3.5 wt.% Ag eutectic alloy. As a contribution to a more complete knowledge of microstructural and thermal properties of Ag-Sn alloys, in the present study two alloys with 10 and 20 % of Ag were prepared and characterized using several experimental techniques. Microstructure of the samples was analyzed by light microscopy. Melting temperatures were measured using differential scanning calorimetry (DSC). Finally, specific heat capacity, thermal diffusivity and thermal conductivity of the investigated alloys were measured by means of xenon-flash technique in the temperature range from 25 to 150 °C.

2. MATERIALS AND METHODS

Two Sn-Ag alloys with 10 and 20 % of Ag were prepared by mixing and melting pieces of pure Sn (99.99%, Alfa Aesar) and Ag (99.99%, Alfa Aesar) in evacuated quartz tubes. Samples were heated at 1000 °C for 30 min. The melts were stirred by shaking the quartz tubes several times to ensure the homogenization of the molten alloys and slowly cooled inside the furnace. The total masses of the prepared samples were about 4 g. The total mass losses of prepared samples were less than 1 mass%, so the nominal compositions of the alloys were accepted for further analysis.

Microstructure analysis of the prepared Sn-Ag alloys was performed by light microscopy using the OLYMPUS GX41 inverted metallographic microscope. Samples were prepared by classic metallographic procedure without etching.

Phase transformations and their heat effects were investigated by using simultaneous thermal analyzer SDT Q600 (TA Instruments). The DSC instrument was calibrated measuring the melting points and the heat of melting of a known mass of standard materials (pure metals: Ag, Bi, In, and Zn). Sample's masses were about 50 mg and heating rate was 5 °Cmin^{-1}. Empty alumina crucible was used as a reference material.

The flash method was applied for determination of thermal diffusivity and thermal conductivity. This method was developed by Parker et al. [7]. A heat source such as laser (laser-flash method) or xenon lump (xenon-flash method) supplies energy pulse to the front face of a thin disk specimen, and the temperature as a function of time at the rear face is automatically recorded. Determination of thermal diffusivity is based on following equation proposed by Parker et al. [7]:

$$\alpha = \frac{1.37L^2}{\pi^2 t_{1/2}} = 0.1388\frac{L^2}{t_{1/2}} \quad \ldots(1)$$

where L represents the thickness of the sample and $t_{1/2}$ is the half-rise time, defined as time interval required for the back-face temperature to reach half of the maximal temperature value.

Thermal diffusivity was measured by using Discovery Xenon Flash (DXF-500) instrument over a range of temperatures from room temperature to 150 °C. For the purpose of thermal diffusivity measurements, the cast Sn-Ag samples were shaped into round disks (12.6 mm in diameter and 2 mm thick with plane-parallel ground end faces) using hydraulic pressing and annealed at 150 °C to relieve internal stresses created during plastic deformation. Samples were placed in a vacuum furnace and heated at a constant rate of 10 °Cmin^{-1} to a measurement temperature. When the furnace temperature was sufficiently stable (temperature changes of less than 1° for 60s) the front surface of the specimen was heated by an energy pulse from the xenon-lamp. Temperatures of rear face of the samples were monitored using the nitrogen-cooled IR detector (InSb sensor).

After the measurements of thermal diffusivity, thermal conductivity of the investigated sample was determined using following fundamental relationship:

$$\lambda = \alpha \cdot \rho \cdot Cp \quad \ldots(2)$$

where λ is thermal conductivity ($Wm^{-1}K^{-1}$), α is thermal diffusivity (m^2s^{-1}), ρ is density (kgm^{-3}), and *C*p is specific heat capacity ($Jg^{-1}K^{-1}$). Alloy density was derived from the measured mass and determined volume of the sample.

3. RESULTS AND DISCUSSION

3.1.Microstructure observation

Fig. 2(a) and (b) illustrates the typical microstructures of the Sn–10%Ag and Sn–20%Ag slowly cooled alloys, which have nearly followed the corresponding equilibrium solidification paths. It can be seen that microstructure of both alloys include large, plate-like, faceted crystals of Ag_3Sn intermetallic compound (bright areas) in the Sn-rich eutectic (dark areas).

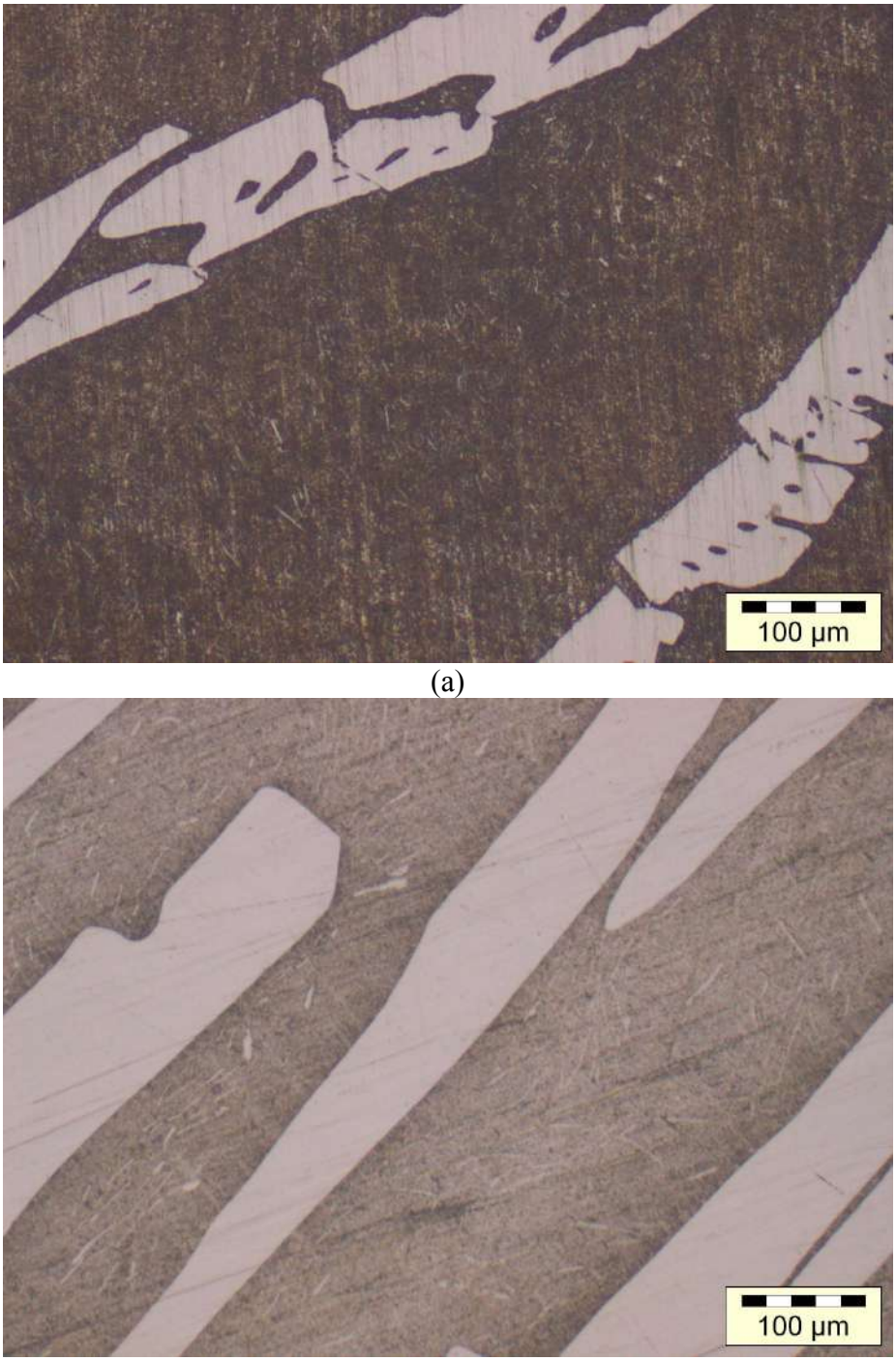

(a)

(b)

Figure 2. Optical image of the microstructure showing plate-like grains of Ag_3Sn phase (bright regions) in the eutectic matrix (dark regions): (a) Sn–10% Ag alloy; (b) Sn–20% Ag alloy

The development of bulk, plate-like crystals of Ag_3Sn intermetallic compound in slowly-cooled eutectic Sn–Ag alloys is attributed to the formation and epitaxial growth of fine eutectic Ag_3Sn crystal nuclei at the leading phase's surfaces of the primary Ag_3Sn crystals due to the match in their crystalline orientation relationship [8]. The formation of plate-like Ag_3Sn crystals has been observed even in the near-eutectic Sn-Ag slowly-cooled alloys [8,9] and it is known that it can adversely affect the plastic deformation properties of the solders [10].

3.2. Differential scanning calorimetry measurements

The analysis of DSC results was done according to the literature recommendations about the interpretation of heat flux DSC thermogram of binary metallic systems [11]. The onset temperature of the first DSC peak in the heating process was considered as the temperature of the invariant eutectic reaction, and the peak temperature of the second thermal effect on heating was selected as the liquidus temperature. DSC heating runs were repeated totally three times and average values were calculated based on the results of repeated tests.

Figs. 3 shows examples of DSC heating curves for the investigated Sn-Ag eutectic alloys.

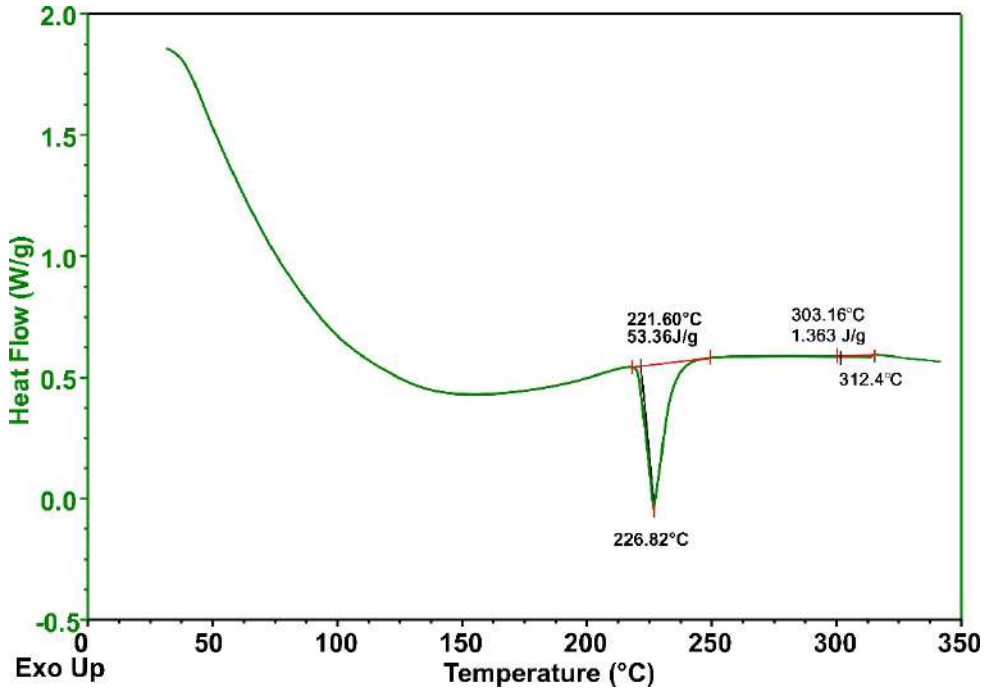

(a)

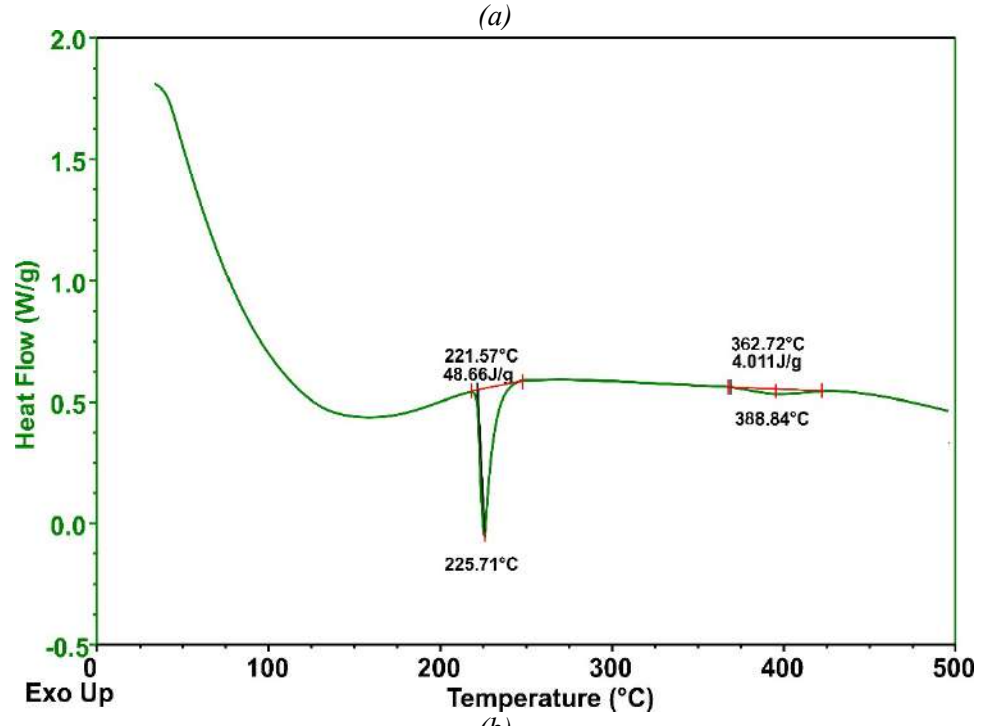

(b)

Figure 3. DSC heating curve: (a) Sn-10% Ag eutectic alloy; (b) Sn-20%Ag

DSC heating scans for both investigated alloys include one sharp endothermic peak related to the apperiance of the (Sn)+ Ag_3Sn→ liquid eutectic reaction. The eutectic reaction denotes the start of the melting for both alloys i.e. their solidus temperature. The measured onset temperature of the eutectic peak is 221.6 °C, which is in excelent agreement with the value of eutectic temperature according to the phase diagram of the Ag-Sn system (221.7 °C) presented in Fig. 1. Besides DSC peaks related to the eutectic reaction, both DSC heating curves include one small peak at higher temperature related to the end of melting of Ag_3Sn primary phase. These peaks are due to the crossing of the liquidus line. The peak temperature for the Sn-10%Ag alloy is 312.4 °C (Fig. 3a), which is in reasonable agreement with the calculated liquidus temperature 316.2 °C. For the Sn-20%Ag alloy, measured liquidus temperature is 388.8 °C (Fig. 3b) and calculated 382.9 °C.
Table 1 presents comparison between experimental results and results of thermodynamic calculation. Average value of eutectic temperature and latent heat of melting together with standard uncertainties evaluated from three repeated tests are presented in Table 1.

Table 1. Comparison between the results of DSC measurements and thermodynamic calculation for the Sn–Ag eutectic alloys

Alloy composition / wt.%	Temperature of eutectic reaction from DSC (°C)	Calculated temperature of eutectic reaction from DSC (°C)	Heat effect of eutectic transition (Jg^{-1})	Experimentally determined liquidus temperature (°C)	Calculated liquidus temperature (°C)
Sn90Ag10	221.6.±0.1	221.7	53.4±0.1	312.4±0.2	316.2
Sn80Ag20	221.6±0.1	221.7	48.7±0.1	388.8±0.3	382.9

3.3.Thermal properties

There are only few studies in literature related to the measurements of specific heat capacity and thermal conductivity for the Sn-Ag alloys. Lloyd et al. [12] reported specific heat capacity value of 0.220 $Jg^{-1}K^{-1}$ at 30 °C for the Sn-3.5% Ag eutectic alloy. The published value of thermal conductivity for the Sn-3.5% Ag eutectic alloy is 78 W/(m·K) at 25 °C[13].
The values of thermal conductivity for pure constitutive metals Ag and Sn are attainable in the reference literature [14]. Thermal conductivity dependences on temperature for pure Ag and low-melting metals Bi, In and Sn are presented in Fig. 4 for comparison. It is known that silver has the highest thermal conductivity of all metals (428.0 $Wm^{-1}K^{-1}$at 20 °C). Tin has moderate thermal conductivity (62.8 $Wm^{-1}K^{-1}$ at 0 °C and 60.7 $Wm^{-1}K^{-1}$ at 100 °C).

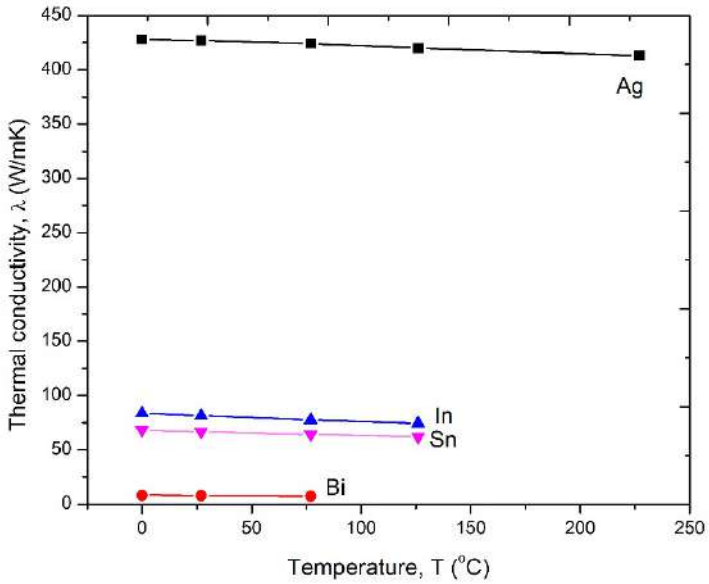

Figure 4. Thermal conductivity of pure polycrystalline metals Ag, Bi, In and Sn as a function of temperature from ref. [14]

In this study, thermal conductivity of solid Sn-Ag alloys has been investigated in the temperature range from 25 to 150 °C using the flash method. The flash technique simultaneously measures thermal diffusivity and specific heat capacity [7,15]. Thermal conductivity can be calculated using the density, thermal diffusivity and specific heat capacity data for the investigated material (Eq. 2).

The obtained values of thermal diffusivity, specific heat capacity and thermal conductivity for the solid Sn-Ag alloys investigated in the temperature range from 25 to 150 °C are given in Table 2. The standard uncertainty (0.68 level of confidence) for the thermal diffusivity measurements is ± 2% [7,16]. For the specific heat capacity measurements, the pure tin was used as a reference material. The standard uncertainty for the specific heat capacity measurements is estimated to be ± 4% [15]. The total standard uncertainty for the thermal conductivity is estimated to be ± 8% [16].

Table 2. Measured specific heat capacity, thermal diffusivity, and thermal conductivity of the investigated Sn–Ag alloys in the temperature range 25-150 °C

Alloy	Temperature (°C)	Specific heat capacity ($Jg^{-1}K^{-1}$)	Thermal diffusivity (mm^2s^{-1})	Thermal conductivity W/(m·K)
Sn-10% Ag	25	0.227	43.86	73.7
	50	0.231	42.74	73.08
	100	0.238	40.24	70.89
	150	0.245	37.81	68.57
Sn-20% Ag	25	0.227	42.44	73.73
	50	0.230	40.71	71.66
	100	0.237	38.45	69.74
	150	0.244	36.21	67.62

From Table 2 it can be noticed that for both investigated alloys specific heat capacity gradually increases while thermal diffusivity and thermal conductivity steadily decrease with increasing temperature. The measured values of specific heat capacity and thermal conductivity for two investigated alloys are close to each other and somewhat higher than those for pure tin. The higher content of silver in the Sn-20% Ag alloy did not result in any significant rice of alloy thermal conductivity. Measured specific heat capacity values of the investigated alloys from this work are in a reasonable agreement with the reported specific heat capacity of the Sn-3.5% Ag eutectic alloy (0.220 $Jg^{-1}K^{-1}$ at 30 °C) [12].

4. CONCLUSION

Based on the obtained results following conclusions can be made:

a) Microstructure of the slowly-cooled Sn-10% Ag and Sn-20% Ag alloys is consisted of long plate-like grains of Ag_3Sn intermetallic phase in the Sn-rich eutectic matrix. According to the previously published studies, the growth of the long plate-like Ag_3Sn crystals is caused by the interaction between fine eutectic Ag_3Sn particles and primary Ag_3Sn particles during slow cooling. Phase fraction of Ag_3Sn phase increases with increasing silver ratio.

b) Solidus and liquidus temperatures of the investigated Sn-Ag alloys were determined by using DSC technique. Measured temperature of eutectic (Sn)+ $Ag_3Sn\rightarrow$ liquid reaction is 221.6 °C, which is in very good agreement with the calculated value. Liquidus temperature inceases and heat of eutectic reaction deacreses with increasing silver ratio.

c) The xenon-flash method was successfully used for the measurements of specific heat capacity, thermal diffusivity and thermal conductivity of the investigated Sn-Ag alloys in the temperature range from 25 to 150 °C. The measured thermal conductivities are slightly higher than thermal conductivity of pure tin and gradually decrease with increasing of temperature. The silver ratio has no significant effect on the thermal conductivity in the investigated composition range.

ACKNOWLEDGEMENT

This work is supported by the Ministry of Education, Science and Technological Development of the Republic of Serbia, project No. OI172037.

5. REFERENCES

[1] KellerJ., BaitherD., WilkeU., SchmitzG.: Acta Materialia, 59 (7) 2731–2741, 2011.
[2] SuganumaK., HuhS.H., KimK., NakaseH., NakamuraY.: Materials Transactions, 42 286-291, 2001.
[3] FimaP.: Applied Surface Science, 257 3265–3268, 2011.
[4] MeydaneriF., SaatciB., OzdemirM.: Kovove Mater. 51 173–181, 2013.
[5] ÇadırlıE., ŞahinM., KayalıR., ArıM., DurmuşS.: Journal of Materials Science: Materials in Electronics, 22(11) 1709-1714, 2011.
[6] KroupaA., DinsdaleA.T., WatsonA., VrestalJ., VízdalJ., ZemanovaA.: JOM, 59 (7) 20-25, 2007.
[7]ParkerW. J., JenkinsR. J., ButlerC. P., AbbottG. L.: J Appl Phys, 32 (9) 1679-1684, 1961.
[8] ShenJ., ChanY.C., LiuS.Y.: Intermetallics 16 1142–1148, 2008.
[9] Shen J, Liu YC, Gao HX, Wei C, Yang Y.Q.: J Electron Mater, 34 (12) 1591-1597, 2005.
[10] Kim KS, Huh S.H., Suganuma K: Mater Sci Eng A,333 (1-2)106-114, 2002.
[11] BoettingerW.J., KattnerU.R., MoonK.W., PerepezkoJ.H.: DTA and Heat-flux DSC Measurements of Alloy Melting and Freezing. In: Zhao JC, ed. Methods for Phase Diagram Determination, Amsterdam: Elsevier Science; 2007, pp. 151-221.
[12] LloydJ.R., ZhangC., TanH.L., ShangguanD., AchariA.: Proceedings of the IEEE/CPMT IEMT Symposium, Austin, TX, USA, 1995, p. 252.
[13] King, J. A.:Material Handbook for Hybrid Microelectronics, Artec House, Norwood, MA, 1988.
[14] Touloukian, Y. S., Powell, R. W., Ho, C. Y., Klemens, P. G.: Thermal Conductivity Metallic Elements and Alloys. Vol. 1. Washington, New York, 1970.

[15] KövérM., BehúlováM., DrienovskýM., MotyčkaP.:Journal of Thermal Analysis and Calorimetry, 122 151-156, 2015.
[16]HuangL., LiuS., DuY., ZhangC.: Calphad, 62 99-108, 2018.